2024 13th International Conference on Electrical and Computer Engineering (ICECE)
December 18–20, 2024, Dhaka, Bangladesh

Fuzzy Rank-Based Ensemble Learning for Eye Disease Classification Using Retinal Images: A Bangladeshi-Specific Dataset with Explainable AI Integration

Shuvashis Sarker
Department of Computer Science and Engineering,
Ahsanullah University of Science and Technology, Dhaka, Bangladesh
*shuvashisofficial@gmail.com

***Abstract*—This study focuses on identifying and categorizing ocular disorders affecting critical components of the eye, including the retina, optic nerve and blood vessels, which can lead to severe outcomes such as visual impairment or blindness if untreated. In Bangladesh, where healthcare resources are scarce, especially in rural regions, early identification of ocular illnesses is crucial to avert permanent vision impairment. To address the deficiency of region-specific datasets, this research employs retinal scans from Bangladeshi healthcare facilities to develop a transfer learning-based solution. Multiple transfer learning models, including DenseNet, EfficientNet, GoogleNet, MobileNet, ResNet50, VGG16, VGG19 and ShuffleNet, have been assessed to determine the best effective architecture for eye illness categorization. A fuzzy rank-based ensemble model was proposed, integrating predictions from these models using the Gompertz function, which adaptively adjusts the weight of each model's predictions to improve classification accuracy. The ensemble model attained an overall accuracy of 96.16%, demonstrating remarkable precision for illnesses such as Diabetic Retinopathy (99.62%) and Disc Oedema (99.63%). Additionally, Explainable AI (XAI) technologies such as LIME have been incorporated to enhance the transparency and interpretability of the model's decision-making process, enabling medical practitioners to understand and verify predictions. By providing a reliable and interpretable AI-based solution, this research significantly improves eye disease diagnosis in Bangladesh, particularly for underserved areas.**

***Index Terms*—Retinal Disease Classification, Transfer Learning (TL), Ensemble Learning (EL), Explainable AI (XAI), Fuzzy Rank-Based Ensemble, Gompertz Function.**

I. Introduction

Eye diseases encompass various conditions affecting the retina, optic nerve, choroid and blood vessels, which can range from chronic to degenerative and potentially lead to blindness if untreated. Conditions such as elevated blood sugar damaging retinal blood vessels [1], increased intraocular pressure (*silent thief of sight*) harming the optic nerve [2] and macular degeneration affecting central vision [3] are significant causes of vision loss. Symptoms like blurred vision and dark spots further impair daily life [4], [5].

In Bangladesh, eye diseases pose a significant public health challenge, particularly in underserved areas where access to healthcare is limited. Over 90% of individuals in Dhaka's slums reportedly suffer from eye conditions, with refractive issues being the most common [6]. Insufficient ophthalmic services and delayed diagnosis exacerbate the risk of irreversible vision impairment [7].

Deep learning (DL) has demonstrated considerable promise in automating the diagnosis and classification of eye diseases through retinal imaging. Convolutional Neural Networks (CNNs) have shown exceptional performance in retinal vascular segmentation and illness prediction tasks. Nevertheless, the majority of current models depend on non-local datasets, which may not adequately reflect the distinct characteristics of Bangladeshi patients, resulting in possible mistakes and biases. Furthermore, whereas ensemble approaches are frequently used worldwide to enhance model robustness and performance, the integration of Ensemble Learning (EL) with Explainable AI (XAI) is not widely implemented, despite its potential to provide transparency and reliability in model predictions.

To bridge this gap, this paper offers a fuzzy rank-based ensemble model with a modified Gompertz function, specifically designed for Bangladeshi retinal data to enhance accuracy and reliability in eye illness categorization. Integrating Explainable AI (XAI) enhances transparency and builds confidence, underscoring the significance of merging EL with XAI for practical and interpretable healthcare solutions. This study makes the following key contributions:

- Utilizes Bangladeshi-specific retinal image data to address an underrepresented dataset.
- Implements transfer learning models for eye disease classification.
- Constructs a fuzzy rank-based ensemble model via a modified Gompertz function.
- Enhances model interpretability through explainable AI (XAI) techniques.

The following portions of the paper are organized as outlined below: Section II discusses Related Works, whereas Section III describes the dataset. Section IV outlines the proposed methodology, whereas Section V clarifies the result analysis. Techniques for Explainable AI are detailed in Section VI, whilst Section VII presents the last observations.

II. Related Works

Recent advances in DL have greatly improved automatic retinal disease detection. This section reviews studies on DL models for retinal disease classification and the use of EL and XAI to enhance model performance and interpretability, categorized into two parts: DL models for classification and the application of EL and XAI.

A. DL Models for Retinal Disease Classification

DL models, particularly CNNs, have been widely used for detecting retinal diseases such as diabetic retinopathy (DR), glaucoma and macular degeneration through fundus images. Khalid et al. [8] introduced FGR-Net, a framework that integrates an autoencoder and classifier to assess and understand the quality of retinal images. It classifies between gradable and non-gradable images, providing visual interpretability, with an accuracy above 89% and an F1-score of 87%, underscoring the importance of quality assessment in retinal imaging. Cen et al. [7] developed a DL platform (DLP) capable of detecting 39 retinal diseases using over 249,620 fundus images. The DLP achieved an AUC of 0.9984, demonstrating high diagnostic accuracy.

To investigate the TL domain, Kallel et al. [9] focused on detecting DR using TL models such as VGG16, VGG19, InceptionV3 and DenseNet169. The InceptionV3 model achieved the highest accuracy of 96.88%. Similarly, Jabbar et al. [10] developed a deep TL-based system for real-time DR detection, achieving 97.6% classification accuracy. This system was particularly designed for remote areas, underscoring the importance of timely diagnosis. Although highly effective for DR, the model does not extend to multiple diseases, a limitation this study seeks to overcome. Lee et al. [11] explored ResNet-18 for differentiating optic atrophy causes such as Leber's hereditary optic neuropathy (LHON) and optic neuritis (ON). The model used Grad-CAM for visualization and achieved an overall accuracy of 93%. Prathibha et al. [12] conducted a comprehensive review of vision-based CAD systems for detecting diabetic retinopathy, highlighting the limitations of current methods and advocating for multi-trait-driven deep learning models to improve accuracy and generalizability.

However, similar to other works, these studies did not incorporate region-specific datasets, which can limit its generalizability to populations like Bangladesh.

B. Ensemble Learning and XAI in Retinal Disease Detection

EL techniques have arisen as a potent instrument for enhancing the precision and resilience of retinal disease detection systems. Li et al. [13] introduced an ensemble approach using multiple improved InceptionV4 models to detect DR and diabetic macular edema (DMO). The model achieved an AUC of 0.992 for DR and 0.994 for DMO, outperforming expert ophthalmologists. Shamrat et al. [14] demonstrated the effectiveness of EL models in improving diagnostic accuracy for retinal diseases. Shamrat's work on DR classification using a novel DRNet13 model achieved 97% accuracy, further highlighting the potential of EL approaches in medical imaging. Naik et al. [15] created an ensemble model that integrates Xception and InceptionV3 with self-attention to categorize OCT pictures into four categories, attaining an accuracy of 96.69%. Their utilization of a U-Net for segmentation surpassed the performance of individual models, underscoring the efficacy of ensemble learning in precise eye disease identification.

XAI has also been a key development in improving the interpretability of DL models. Faria et al. [16] investigated the use of various DL models and XAI techniques such as Grad-CAM, Grad-CAM++ and LayerCAM. These methods provided transparency in model predictions, highlighting critical areas in retinal images that contribute to the classification process. It achieved a high accuracy of 94.17% using ResNet101 for classification tasks. Lee et al. [11] used Grad-CAM to generate heatmaps that visualize the regions in retinal images contributing to disease predictions. This method enhances the interpretability of the model, ensuring that clinicians can understand how the model arrives at its decisions. Similarly, Pandey et al. [17] used a deep convolutional ensemble (DCE) model to classify multiple retinal diseases, achieving higher accuracy than ophthalmologists in certain categories. The DCE approach is aligned with the fuzzy rank-based ensemble model proposed in this study, but this research builds on it by using XAI and region-specific data.

From the related work reviewed, it is evident that XAI has rarely been applied in ensemble methods, particularly for region-specific datasets. Despite the success of DL and EL in retinal disease detection, a gap exists due to the lack of region-specific data and the underutilization of XAI techniques in these models. This study addresses these gaps by utilizing Bangladeshi retinal data with a fuzzy rank-based ensemble model, ensuring both accuracy and interpretability through XAI techniques. By rectifying this imbalance, the study offers valuable insights for clinicians in underserved regions, improving trust, transparency, and clinical decision-making.

III. Dataset

A. Dataset Collection

The dataset was collected from "*Anwara Hamida Eye Hospital*" and "*BNS Zahrul Haque Eye Hospital*" in the Faridpur district, comprising 5335 retinal images of both healthy and affected eyes. These images were verified by domain experts to ensure accurate diagnostic labels. Figure 1 shows sample images from each disease category.

B. Dataset Overview

The dataset includes images of various eye diseases, such as "*Retinitis Pigmentosa*", "*Retinal Detachment*", "*Pterygium*",

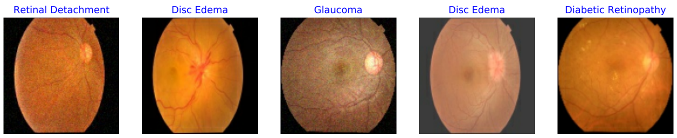

Fig. 1: Sample Images of the dataset

"*Myopia*", "*Macular Scar*", "*Glaucoma*", "*Disc Edema*", "*Diabetic Retinopathy*" and "*Central Serous Chorioretinopathy*", alongside *Healthy* eye images. Figure 2 illustrates the class distribution. This diverse dataset is essential for developing models for detecting and classifying eye diseases, addressing the need for early detection in regions like Bangladesh. The dataset is available on *Mendeley Data* [18].

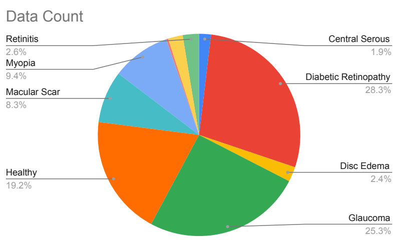

Fig. 2: Various Class Density of the Dataset

IV. Methodology

A. Data Preprocessing

During the preprocessing phase, two essential strategies are employed to ready the dataset for training. The Synthetic Minority Over-sampling Technique (SMOTE) is employed to rectify class imbalance by augmenting the minority classes, hence creating a more equitable dataset for training. Subsequent to balancing the dataset, data augmentation techniques are utilized to enhance the dataset further. Images are first resized to 128x128 pixels and normalized using min-max normalization. Augmentation is then applied, including horizontal flipping, adding Gaussian noise, adjusting contrast and brightness and randomly rotating images between -15 and +15 degrees.These augmentation strategies facilitate the generation of numerous permutations of each image, hence boosting the model's robustness. After preprocessing, the dataset is partitioned into training, validation, and test sets in an 80-10-10 ratio to enable balanced model evaluation. Figure 3 illustrates the overall process of the data preprocessing steps.

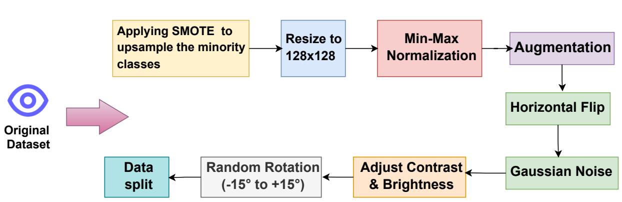

Fig. 3: Different Data Preprocessing steps

B. Model Architecture

The proposed model architecture utilizes multiple renowned pre-trained models, such as GoogLeNet, Inception_v3, ResNet50, DenseNet and MobileNet, all of which have been pre-trained using the ImageNet dataset. Figure 4 depicts the architecture and ensemble methodology of the proposed model. These models are fine-tuned to suit the specific task of eye disease classification. The architecture begins by using the pre-trained layers for feature extraction and a custom classifier which is added on top. The classifier consists of a sequential model with a flattening layer followed by multiple dense layers with ReLU activation and dropout regularization to prevent overfitting. The classifier incorporates a 50% dropout prior to and subsequent to the initial dense layer of 1024 units, followed by a second dense layer with 512 units and a 25% dropout preceding the final output layer, which categorizes the images into several disease groups. To enhance accuracy, a fuzzy rank-based ensemble method has employed, which integrates the predictions from multiple models using a modified Gompertz function. This ensemble approach improves the model's robustness and mitigates misclassifications, providing a more reliable system for eye disease detection.

C. Fuzzy Rank-based Ensemble Method

The fuzzy rank-based ensemble method improves upon traditional ensemble techniques by dynamically adjusting the contribution of each model's prediction for individual test cases, rather than relying on static weights. This method enhances classification accuracy by considering the prediction scores from each base model for every test sample separately. A modified Gompertz function is employed to improve these scores, enabling effective management of each model's contribution. The Gompertz function is expressed as:

$$f(t) = ae^{-e^{b-ct}}$$

In this context, a denotes the asymptote, b governs the displacement along the x-axis, c modifies the y-axis, and e represents Euler's number. Fuzzy ranks are then generated for each class based on the model's confidence, ensuring that predictions are more accurate and reliable. If a class does not rank within the top predictions, a penalty is imposed, further refining the classification process. The final decision is made by multiplying the fuzzy rank and confidence factors, selecting the class with the highest combined score. This method ensures more flexible and adaptable classification by dynamically adjusting ranks for each test sample, improving overall performance and robustness without needing to manually modify model weights across different datasets [19].

V. Result Analysis

A. Experimental Setup

The experiments are conducted using a Ryzen 5 3600 processor, NVIDIA GeForce RTX 3060 Ti 8GB GPU, and 32GB of RAM. Models are implemented in PyTorch with a learning rate of 1e-4 and trained for 30 epochs. CrossEntropyLoss have

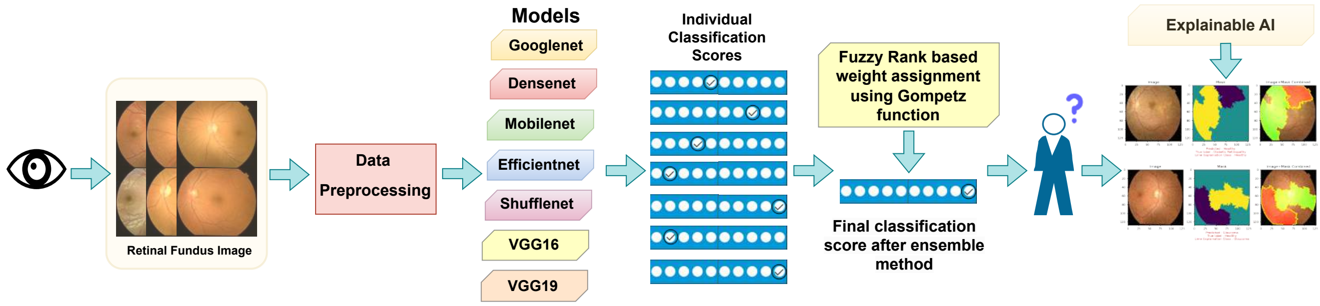

Fig. 4: Workflow of Proposed Method

TABLE I: Measures of Performance for Various TL Models

Model	Accuracy	Precision	Recall	F1-score
Densenet	0.9589	0.9591	0.9594	0.9591
EfficientNet	**0.9595**	**0.9596**	**0.9594**	**0.9597**
Googlenet	0.9474	0.9485	0.9494	0.9488
MobileNet	0.9565	0.9566	0.9568	0.9560
ResNet50	0.9491	0.9505	0.9518	0.9510
VGG16	0.9545	0.9541	0.9551	0.9545
VGG19	0.9498	0.9509	0.9519	0.9514
ShuffleNet	0.9191	0.9210	0.9227	0.9214

used for multi-class classification, and the Adam optimizer ensures fast, stable convergence. This setup maximized model performance and ensures robust results.

B. Performance Discussion

The result analysis from Table I shows that EfficientNet and Densenet are the best-performing models for eye disease classification. EfficientNet has the highest accuracy at 0.9595, followed closely by Densenet with 0.9589. Both models have done a great job of capturing important features from the dataset. Table I also shows that MobileNet and VGG16 have also performed well, with accuracies of 0.9565 and 0.9545. ResNet50, VGG19, and GoogLeNet have achieved slightly lower accuracies around 0.949, while ShuffleNet V2 has the lowest accuracy at 0.9191, making it less suitable for this task. Figure 5 illustrates the accuracy and loss curves for EfficientNet and Densenet. Both models have showed steady improvement in accuracy and a decrease in loss during training, which means they learned well from the data and are stable throughout the process. These two models, especially EfficientNet, have stood out as the most reliable for classifying eye diseases based on their strong performance and ability to handle the dataset effectively. MobileNet and VGG16 have also performed well, but EfficientNet and Densenet have proven to be the best choices for this task.

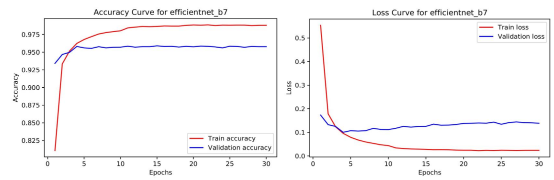

(a) Efficientnet Training Curves

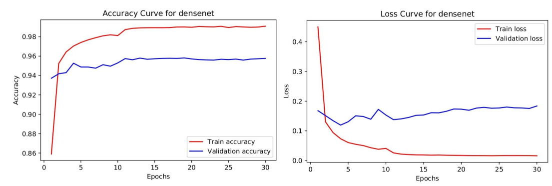

(b) Densenet Training Curves

Fig. 5: Training and validation curves.

C. Effectiveness of Ensemble Method

This work employs an ensemble method that utilizes fuzzy rankings to improve classification accuracy by amalgamating the outputs of multiple pre-trained models. Specifically, the models used are EfficientNet, Densenet and other TL models, as detailed in the previous sections. The predictions from these models for each test sample are stored, and fuzzy ranks are assigned to the top classes. The Gompertz function dynamically adjusts the weight of each model's predictions, allowing the ensemble to balance contributions based on performance. This ensures that top-performing predictions are given higher weights, while less relevant ones are penalized, refining the final classification output. The ensemble model generates the final classification scores across multiple eye disease classes, as shown in Table II. This table presents the performance parameters, encompassing precision, recall and F1-score for each class, alongside an overall accuracy of 96.16%. Among the classes, diseases like Diabetic Retinopathy and Disc Edema show high precision and recall, indicating the model's effectiveness in accurately identifying these conditions.

Figure 6 presents the confusion matrix and ROC curve for the ensemble method. The confusion matrix displays the classification accuracy across different eye disease classes, while the ROC curve highlights the model's ability to distinguish between these classes. With an AUC close to 1 for most classes, the ensemble method demonstrates high accuracy and robustness in eye disease classification.

VI. Explainable AI(XAI)

Explainable AI (XAI) is essential for improving the transparency and interpretability of deep learning models, espe-

TABLE II: Performance Metrics across Various Classes using the Ensemble Method

Class	Precision	Recall	F1-score
Central Serous Chorioretinopathy	0.9698	0.9945	0.9820
Diabetic Retinopathy	0.9962	0.9835	0.9898
Disc Edema	0.9963	0.9982	0.9972
Glaucoma	0.8891	0.8818	0.8854
Healthy	0.8812	0.8873	0.8842
Macular Scar	0.9755	0.9469	0.9610
Myopia	0.9642	0.9872	0.9756
Pterygium	0.9982	0.9891	0.9936
Retinal Detachment	0.9871	0.9799	0.9835
Retinitis Pigmentosa	0.9779	0.9944	0.9860
Accuracy		0.9616	
Macro Avg	0.9663	0.9673	0.9668
Weighted Avg	0.9557	0.9556	0.9556

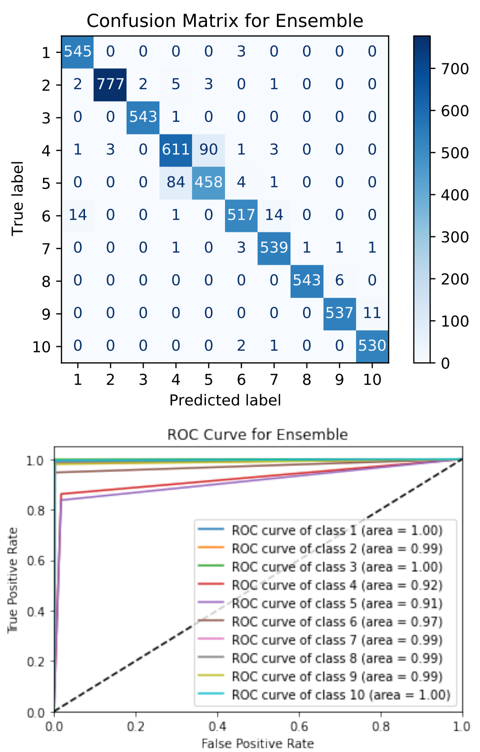

Fig. 6: Visualization of the ensemble method's performance

cially neural networks, which are sometimes seen as "black boxes" because of their intricate decision-making mechanisms. In healthcare, where misclassifications can have serious consequences, understanding model predictions is crucial. XAI helps bridge the gap between AI models and medical professionals by providing clear insights into the reasoning behind predictions, building trust and improving decision-making. LIME [20] is a key XAI technique that clarifies how complex models, like classifiers and regressors, make predictions. LIME works by locally approximating the original model with a simpler, interpretable version and can be applied across various data types. It creates artificial data points, predicts classes, and uses a linear model to highlight the most significant features, making AI predictions easier to understand and validate [21].

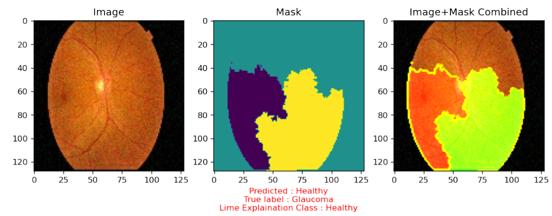

(a) Predicted: Healthy, True: Glaucoma

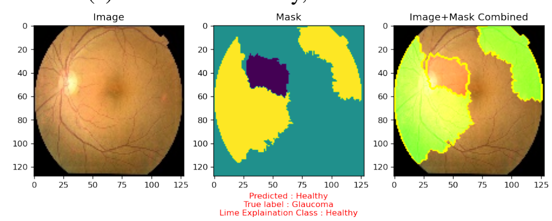

(b) Predicted: Healthy, True: Glaucoma

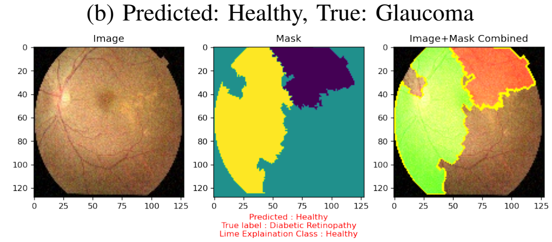

(c) Predicted: Healthy, True: Diabetic Retinopathy

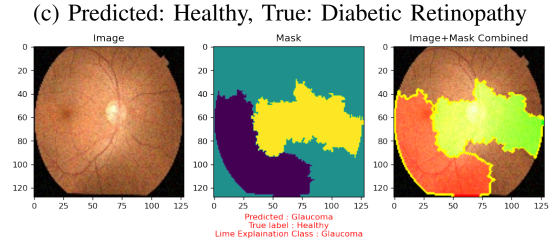

(d) Predicted: Glaucoma, True: Healthy

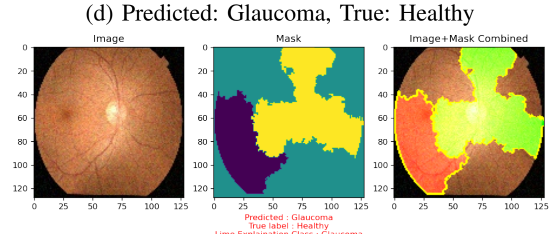

(e) Predicted: Glaucoma, True: Healthy

Fig. 7: Some sample images of misclassifications by the model

Figure 7 shows the misclassified images which is analyzed using LIME, providing insights into the model's misinterpretations. Figure 7a shows the model incorrectly predicting a healthy eye when the true label was glaucoma. The green regions, where the model focused, represent areas it associated with healthy features, while the red areas, indicative of other classes, are not significant enough to guide the model towards the correct glaucoma classification. In Figure 7b, the model has again predicted a healthy eye, but the true label is glaucoma. The LIME explanation highlights green areas where the model have found patterns similar to a healthy eye, leading to the misclassification, as it overlooked the crucial features of glaucoma. Similarly, in Figure 7c, the model has misclassified diabetic retinopathy as healthy. The green regions reflect areas the model associated with a healthy eye, while the red regions, representing disease-related features, are ignored, leading to the wrong classification. In Figure 7d and Figure 7e, the model has predicted glaucoma, but the true labels are healthy. The green regions in these images are interpreted by the model as indicative of glaucoma, while the actual healthy features are disregarded, resulting in misclassification. These LIME explanations demonstrate how the model incorrectly prioritized certain regions, causing it to misclassify the images compared to their true labels.

VII. Conclusion

This research introduces a DL methodology for the identification and categorisation of ocular illnesses utilising a retinal imaging dataset particular to Bangladesh. The proposed strategy, utilising a fuzzy rank-based ensemble model in conjunction with the Gompertz function, achieves a remarkable accuracy of 96.16%, proficiently recognising conditions such as Diabetic Retinopathy and Disc Oedema with notable precision. The application of Explainable AI approaches like LIME enhances transparency, enabling medical professionals to comprehend the model's predictions more effectively. The dependence on a regional dataset constrains the model's generalisability, potentially diminishing it's efficacy on datasets from other regions with distinct population features. Future endeavours seek to apply this model in real-world healthcare environments, improving its precision by integrating larger, more varied datasets and investigating further methodologies in model optimisation and interpretability. The objective is to enhance the model to yield more dependable forecasts and elucidate explanations, so rendering it a significant asset in practical clinical applications.

References

[1] Y. Jang, J. Son, K. H. Park, S. J. Park, and K.-H. Jung, "Laterality classification of fundus images using interpretable deep neural network," *Journal of digital imaging*, vol. 31, pp. 923–928, 2018.

[2] Y. Pan, J. Liu, Y. Cai, X. Yang, Z. Zhang, H. Long, K. Zhao, X. Yu, C. Zeng, J. Duan, *et al.*, "Fundus image classification using inception v3 and resnet-50 for the early diagnostics of fundus diseases," *Frontiers in Physiology*, vol. 14, p. 1126780, 2023.

[3] M. Mateen, J. Wen, Nasrullah, S. Song, and Z. Huang, "Fundus image classification using vgg-19 architecture with pca and svd," *Symmetry*, vol. 11, no. 1, p. 1, 2018.

[4] Y. Katada, N. Ozawa, K. Masayoshi, Y. Ofuji, K. Tsubota, and T. Kurihara, "Automatic screening for diabetic retinopathy in interracial fundus images using artificial intelligence," *Intelligence-Based Medicine*, vol. 3, p. 100024, 2020.

[5] W. L. Alyoubi, M. F. Abulkhair, and W. M. Shalash, "Diabetic retinopathy fundus image classification and lesions localization system using deep learning," *Sensors*, vol. 21, no. 11, p. 3704, 2021.

[6] I. Sutradhar, P. Gayen, M. Hasan, R. D. Gupta, T. Roy, and M. Sarker, "Eye diseases: the neglected health condition among urban slum population of dhaka, bangladesh," *BMC ophthalmology*, vol. 19, pp. 1–8, 2019.

[7] L.-P. Cen, J. Ji, J.-W. Lin, S.-T. Ju, H.-J. Lin, T.-P. Li, Y. Wang, J.-F. Yang, Y.-F. Liu, S. Tan, *et al.*, "Automatic detection of 39 fundus diseases and conditions in retinal photographs using deep neural networks," *Nature communications*, vol. 12, no. 1, p. 4828, 2021.

[8] S. Khalid, H. A. Rashwan, S. Abdulwahab, M. Abdel-Nasser, F. M. Quiroga, and D. Puig, "Fgr-net: interpretable fundus image gradeability classification based on deep reconstruction learning," *Expert Systems With Applications*, vol. 238, p. 121644, 2024.

[9] F. Kallel and A. Echtioui, "Retinal fundus image classification for diabetic retinopathy using transfer learning technique," *Signal, Image and Video Processing*, vol. 18, no. 2, pp. 1143–1153, 2024.

[10] A. Jabbar, S. Naseem, J. Li, T. Mahmood, K. Jabbar, A. Rehman, and T. Saba, "Deep transfer learning-based automated diabetic retinopathy detection using retinal fundus images in remote areas," *International Journal of Computational Intelligence Systems*, vol. 17, no. 1, pp. 1–20, 2024.

[11] D. K. Lee, Y. J. Choi, S. J. Lee, H. G. Kang, and Y. R. Park, "Development of a deep learning model to distinguish the cause of optic disc atrophy using retinal fundus photography," *Scientific Reports*, vol. 14, no. 1, p. 5079, 2024.

[12] S. Prathibha *et al.*, "Advancing diabetic retinopathy diagnosis with fundus imaging: A comprehensive survey of computer-aided detection, grading and classification methods," *Global Transitions*, vol. 6, pp. 93–112, 2024.

[13] F. Li, Y. Wang, T. Xu, L. Dong, L. Yan, M. Jiang, X. Zhang, H. Jiang, Z. Wu, and H. Zou, "Deep learning-based automated detection for diabetic retinopathy and diabetic macular oedema in retinal fundus photographs," *Eye*, vol. 36, no. 7, pp. 1433–1441, 2022.

[14] F. J. M. Shamrat, R. Shakil, B. Akter, M. Z. Ahmed, K. Ahmed, F. M. Bui, M. A. Moni, *et al.*, "An advanced deep neural network for fundus image analysis and enhancing diabetic retinopathy detection," *Healthcare Analytics*, vol. 5, p. 100303, 2024.

[15] G. Naik, N. Narvekar, D. Agarwal, N. Nandanwar, and H. Pande, "Eye disease prediction using ensemble learning and attention on oct scans," in *Future of Information and Communication Conference*, pp. 21–36, Springer, 2024.

[16] F. T. J. Faria, M. B. Moin, P. Debnath, A. I. Fahim, and F. M. Shah, "Explainable convolutional neural networks for retinal fundus classification and cutting-edge segmentation models for retinal blood vessels from fundus images," *arXiv preprint arXiv:2405.07338*, 2024.

[17] P. U. Pandey, B. G. Ballios, P. G. Christakis, A. J. Kaplan, D. J. Mathew, S. O. Tone, M. J. Wan, J. A. Micieli, and J. C. Wong, "Ensemble of deep convolutional neural networks is more accurate and reliable than board-certified ophthalmologists at detecting multiple diseases in retinal fundus photographs," *British Journal of Ophthalmology*, vol. 108, no. 3, pp. 417–423, 2024.

[18] M. R. Rashid, S. Sharmin, T. Khatun, M. Z. Hasan, and M. S. Uddin, "Eye disease image dataset." https://data.mendeley.com/datasets/s9bfhswzjb/1, 2024. Version 1, Published: 2 April 2024, Accessed: 2024-10-05.

[19] K. K. Sahoo, I. Dutta, M. F. Ijaz, M. Woźniak, and P. K. Singh, "Tlefuzzynet: fuzzy rank-based ensemble of transfer learning models for emotion recognition from human speeches," *IEEE Access*, vol. 9, pp. 166518–166530, 2021.

[20] M. T. Ribeiro, S. Singh, and C. Guestrin, "" why should i trust you?" explaining the predictions of any classifier," in *Proceedings of the 22nd ACM SIGKDD international conference on knowledge discovery and data mining*, pp. 1135–1144, 2016.

[21] V. Vimbi, N. Shaffi, and M. Mahmud, "Interpreting artificial intelligence models: a systematic review on the application of lime and shap in alzheimer's disease detection," *Brain Informatics*, vol. 11, no. 1, p. 10, 2024.